

NEW PRINCIPLE FOR MISSILE GUIDANCE AND CONTROL

Shinar Josef¹,

Technion, Israel Institute of Technology, Haifa, 32000 Israel

Keywords: *interception, estimation, guidance*

Abstract

Motivated to allow efficient ballistic missiles defense, the paper describes a recently developed integrated estimation/guidance design paradigm based on several innovative concepts that provides robust satisfactory homing performance against randomly maneuvering targets. The new paradigm was developed and tested first by using a simplified planar constant speed interception scenario model. In this paper the integrated estimation/guidance algorithm is validated by simulations of generic endo-atmospheric theatre ballistic missile defense interception scenarios against two types of stressing random target maneuvers.

1. Introduction

Historically, guided interceptor missiles were designed against aircraft type targets, with clear speed and maneuverability advantage of the missile. Due to the vulnerability of an aircraft structure, miss distances compatible with the lethal radius of the missile warhead, were admissible. Current warfare concepts involve the interception of tactical ballistic missiles (TBM), attacking high value targets (probably with unconventional warheads). Such scenario has presented an extreme challenge to the guided missile community. TBMs fly at very high speeds and their atmospheric maneuvering potential, which can be made useful by a modest technical effort, is comparable to that of the interceptors. Successful interception of a TBM requires a small miss distance or even a direct

hit. Such accuracy against targets flying on ballistic trajectories was recently demonstrated [1-2]. However, recent studies indicated [3-4] that currently used guidance and estimation methods are unable to guarantee satisfactory guidance accuracy against highly maneuvering targets expected in the future.

All 'modern' missile guidance laws used at the present were developed based on a linearized kinematical model and a linear quadratic optimal control concept (with unbounded control). Thus, the limited maneuver potential of the interceptor has not been taken into account. These guidance laws have included the effects of non ideal dynamics of the guidance system and the contribution of target maneuvers in the 'generalized zero effort miss distance' and used a time varying gain schedule [5]. For the contribution of the target maneuvers, their current value and future evolution must be known. The information on the current target maneuver, since it cannot be directly measured, has to be obtained by an observer (since in effect the measurements are noise corrupted, by an estimator). For the future evolution in most cases, a constant target maneuver has been assumed. Theoretically, if the assumption on the target behavior is correct, the measurements are ideal and the lateral acceleration of the interceptor does not saturate, such a guidance law can reduce the miss distance to zero. In practice, if the interceptor/target maneuver ratio is sufficiently high, the inevitable saturation occurs only very near to the end and the resulting miss distance becomes negligibly small.

A multi-year investigation has been conducted at the Faculty of Aerospace Engineering of the Technion to identify and

¹ Professor Emeritus, Faculty of Aerospace Engineering. Fellow AIAA.

correct the deficiencies of the conservative common practice in interceptor guidance law design. This investigation resulted in developing an integrated estimation/guidance design paradigm, based on several innovative concepts, providing robust satisfactory homing performance against randomly maneuvering targets. The ideas involved in the revolutionary design concept were developed and tested first by using a simplified linearized planar constant speed interception scenario model [6].

The objective of this paper is to outline the concept and to report the validation of the integrated estimation/guidance algorithm in generic, but realistic 3D nonlinear endo-atmospheric theatre ballistic missile defense scenarios against two types of the most stressing random target maneuvers.

2. Problem Statement

2.1 Scenario description

Two scenarios of intercepting randomly maneuvering TBMs are considered. The first one is a three-dimensional endo-atmospheric ballistic missile defense (BMD) scenario with time-varying parameters (velocities and acceleration limits). Due to the complexity and the large number of variable parameters such a scenario is not convenient for developing and testing new ideas. For the sake of research efficiency (simplicity, repeatability and reduced computational load), a simplified planar constant speed model was used in the analytical development task. The more complex generic BMD scenario was used for validation.

In both scenarios, the homing endgame starts as the onboard seeker of the interceptor succeeds to “lock on” the target. The relative geometry is near a head-on engagement. It is assumed that at this moment the initial heading error, with respect to a collision course, is small and neither the interceptor nor the target is maneuvering. These assumptions allow the linearization of the interception geometry and the decoupling the three-dimensional equations of motion in two identical sets in perpendicular planes.

2.2 Information structure

It is assumed that the interceptor measures range and range-rate with good accuracy, allowing to compute the time-to-go. However, the measurements of the line of sight angle are corrupted by a zero mean white Gaussian angular noise. The interceptor’s own acceleration is accurately measured, but the target acceleration has to be estimated based on the available measurements. The target has no information on the interceptor, but, being aware of an interception attempt, it can start applying evasive maneuvers at any time, randomly changing the direction of the maneuver.

2.3 Lethality model

The objective of the interception is the destruction of the target. The probability of destroying the target is determined by the following simplified lethality function,

$$P_d = \begin{cases} 1, & M \leq R_k, \\ 0, & M > R_k, \end{cases} \quad (1)$$

where R_k is the lethal (kill) radius of the warhead and M is the miss distance.

2.4 Performance index

The natural (deterministic) cost function of the interception engagement is the miss distance. Due to the noisy measurements and the random target maneuvers, the miss distance is a random variable with an a priori unknown probability distribution function. Based on the lethality function (1), the efficiency of a guided missile strongly depends on the lethal radius R_k of its warhead. One of the possible figures of merit is the single shot kill probability (SSKP) for a given warhead, defined by

$$SSKP = E \{P_d (R_k)\} \quad (2)$$

where E is the mathematical expectation taken over the entire set of noise samples against any

given feasible target maneuver. The objective of the guidance is to maximize this value. An alternative figure of merit is the smallest possible lethal radius R_k that guarantees a predetermined probability of success. In several recent studies [3, 4, 6] the required probability of success has been assumed as 0.95, yielding the following performance index

$$J = R_k = \arg \{SSKP = 0.95\} \quad (3)$$

In addition to these two crisp measures a large number of Monte Carlo simulations can provide the cumulative probability distribution function of the miss distance for comparing the homing performances of different guidance systems.

2.5 Equations of planar motion

The analysis of a planar interception endgame is based on the following set of simplifying assumptions:

- (i) The engagement between the interceptor (*pursuer*) and the maneuvering target (*evader*) takes place in a plane.
- (ii) Both the interceptor and the maneuvering target have constant speeds V_j and bounded lateral accelerations $|a_j| < (a_j)^{\max}$ ($j = E, P$).
- (iii) The maneuvering dynamics of both vehicles can be approximated by first order transfer functions with time constants τ_P and τ_E , respectively.
- (iv) The relative interception trajectory can be linearized with respect to the initial line of sight.

In Fig. 1 a schematic view of the endgame geometry is shown. The aspect angles ϕ_P and ϕ_E are small, so the approximations $\cos(\phi_i) \approx 1$ and $\sin(\phi_i) \approx (\phi_i)$, ($i = P, E$), are valid and coherent with assumption (iv). Based on these assumptions the final time of the interception can be computed for any given initial range R_0 of the endgame

$$t_f = R_0 / (V_P + V_E), \quad (4)$$

allowing to define the time-to-go by

$$t_{go} = t_f - t \quad (5)$$

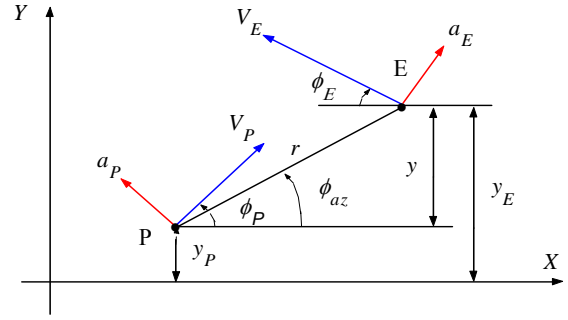


Figure 1. Planar interception geometry

The state vector in the equations of relative motion normal to the reference line is

$$\mathbf{X}^T = (x_1, x_2, x_3, x_4) = (y, dy/dt, a_E, a_P) \quad (6)$$

where

$$y(t) \triangleq y_E(t) - y_P(t) \quad (7)$$

The corresponding equations of motion and the respective initial conditions are

$$\dot{x}_1 = x_2; \quad x_1(0) = 0 \quad (8)$$

$$\dot{x}_2 = x_3 - x_4; \quad x_2(0) = V_E \phi_{E0} - V_P \phi_{P0} \quad (9)$$

$$\dot{x}_3 = (a_E^c - x_3)/\tau_E; \quad x_3(0) = 0 \quad (10)$$

$$\dot{x}_4 = (a_P^c - x_4)/\tau_P; \quad x_4(0) = 0 \quad (11)$$

where a_E^c and a_P^c are the commanded lateral accelerations of the target (*evader*) and the interceptor (*pursuer*) respectively.

$$a_E^c = a_E^{\max} \mathbf{v}; \quad |\mathbf{v}| \leq 1 \quad (12)$$

$$a_P^c = a_P^{\max} \mathbf{u}; \quad |\mathbf{u}| \leq 1 \quad (13)$$

The non zero initial conditions $V_E \phi_{E0}$ and $V_P \phi_{P0}$ represent the respective initial velocity component not aligned with the initial (reference) line of sight. By assumption (iv) these components are small compared to the components along the line of sight.

The set of equations (8)-(13) can be written in a compact form as a linear, time dependent, vector differential equation

$$\dot{X} = A(t) X + B(t) \mathbf{u} + C(t) \mathbf{v} \quad (14)$$

The problem involves two non-dimensional parameters of physical significance: the interceptor/target maximum maneuverability ratio

$$\mu \triangleq (a_p)^{\max} / (a_e)^{\max} \quad (15)$$

and the ratio of the target/interceptor time constants

$$\varepsilon \triangleq \tau_e / \tau_p \quad (16)$$

The miss distance (the deterministic cost function of the interception) can be written as

$$J = |DX(t_f)| = |x_1(t_f)| \quad (17)$$

where

$$D = (1, 0, 0, 0) \quad (18)$$

2.6 Problem formulation

There is a basic deficiency in formulating the interception of a maneuverable target as an *optimal control* problem. Since target maneuvers are independently controlled, future target maneuver time history (or strategy) cannot be predicted, the *optimal control* formulation is not appropriate. The scenario of intercepting a maneuverable target has to be formulated as a *zero-sum differential game of pursuit-evasion*. In such a formulation, there are two independent controllers and the cost function is minimized by one of them and maximized by the other. By using such formulation, several deterministic zero-sum pursuit-evasion game models were solved. These game solutions provided simultaneously the interceptor's guidance law (*the optimal pursuer strategy*), the "worst" target maneuver (*the optimal evader strategy*) and the resulting guaranteed miss distance (the saddle-point *value* of the game). Two optimal guidance laws based

on perfect information linear game solutions with bounded controls are briefly described in the sequel.

3 Game Optimal Guidance Laws

3.1 DGL/1.

The first *perfect information* model solved was of time invariant game parameters [7]. The set of assumptions (i) – (iv) allowed casting the problem to the canonical form of linear games, from which a reduced order game with only a single state variable, the *zero effort miss distance*, denoted by Z , was obtained. As the independent variable of the problem, the time-to-go (t_{go}), defined by (5), was selected. The solution of this game is determined by the two parameters μ and ε defined by (15) and (16). The explicit expression for Z is

$$Z = x_1 + x_2 t_{go} - \Delta Z_P + \Delta Z_E \quad (19)$$

with

$$\Delta Z_P = x_3 (\tau_p)^2 [\exp(\tilde{\theta}_P) + \theta_P - 1] \quad (20)$$

$$\Delta Z_E = x_4 (\tau_e)^2 [\exp(\tilde{\theta}_E) + \theta_E - 1] \quad (21)$$

where $\theta_P = t_{go} / \tau_P$ and $\theta_E = t_{go} / \tau_E$.

The game solution results in the decomposition of the reduced space (t_{go}, Z) into two regions of different strategies, as it can be seen in Fig. 2. These regions are separated by the pair of optimal boundary trajectories denoted respectively by Z^*_+ and Z^*_- , reaching tangentially the $Z = 0$ axis at $(t_{go})_s$, where $(t_{go})_s$ is the non zero root of the equation $dZ/dt_{go} = 0$. One of the regions is a *regular* one, denoted by D_I , where the optimal strategies of the players are of the "bang-bang" type

$$\mathbf{u}^* = \mathbf{v}^* = \text{sign} \{Z\} \quad \forall Z \neq 0 \quad (22)$$

\mathbf{u} and \mathbf{v} being the normalized controls of the *pursuer* (interceptor) and the *evader* (the maneuvering target) respectively. The *value* of the game in this region is a unique function of the initial conditions.

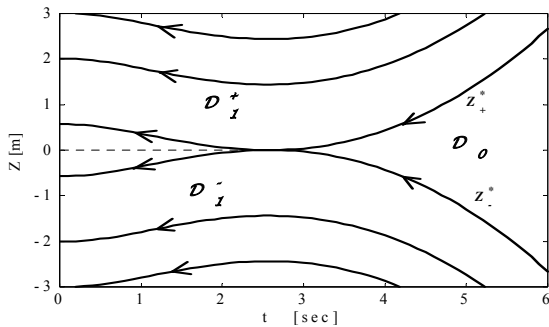


Fig. 2. Decomposition of the reduced game space.

The boundary trajectories themselves also belong to D_I . Inside the other region, denoted by D_0 , the optimal strategies are arbitrary and the value of the game is constant, depending on the parameters of the game (μ, ϵ). If the parameters of the game are such that $\mu\epsilon \geq 1$, then the only root of the equation $dZ/dt_{go} = 0$ is zero and the value of the game in D_0 is also zero. Note that the “bang-bang” strategies (22) are also optimal in D_0 .

The practical interpretation of this game solution is the following: (i) the optimal missile guidance law can be selected as (22) during the entire end game; (ii) the worst target maneuver is a constant lateral acceleration starting not after $(t_{go})_s$; (iii) the guaranteed miss distance depends on the parameters (μ, ϵ) and can be made zero if $\mu\epsilon \geq 1$. In this case, D_0 , which includes all initial conditions of practical importance, becomes the capture zone of this game. Implementation of the optimal missile guidance law, denoted as DGL/1, requires the perfect knowledge of the zero effort miss distance, which includes also the current lateral acceleration of the target.

3.2 DGL/E.

The second model is also a planar one, but with time varying velocities and maneuverabilities. In this perfect information game, assumption (ii) is replaced by assuming that profiles of these variables are known along a nominal trajectory. Such a model is suitable for the analysis of a realistic BMD scenario. The solution of this game [8], is qualitatively similar to the previous

one, but depends strongly on the respective profiles of the velocity/maneuverability and obviously, the value of μ is not constant. Due to the time varying profiles, the expressions of the zero effort miss distance, as well as of $(t_{go})_s$ and the guaranteed miss distance, become more complex. In spite of this (algebraic) complexity, the implementation of the optimal missile guidance law, denoted as DGL/E, doesn't present essential difficulties, although it requires the velocity and maneuverability profiles in the endgame that can be precalculated along a nominal trajectory.

3.3 Implementation with noisy measurements

As already mentioned, the implementation of the perfect information guidance laws DGL/1 and DGL/E requires the knowledge of the target lateral acceleration. Since this variable cannot be directly measured, it has to be estimated based on noise corrupted measurements. If the pursuer uses DGL/1, derived from the perfect information game solution [7], the evader can take advantage of the estimation delay and achieve a large miss distance by adequate optimal maneuvering [9], even if the game parameters are such that the guaranteed miss distance should be zero, as it is illustrated in Fig. 3.

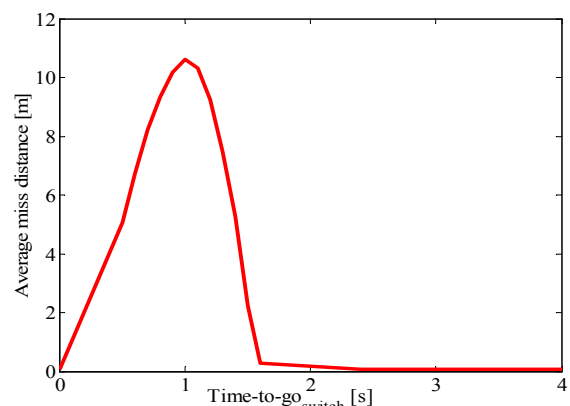


Fig. 3. Homing performance of DGL/1 against “bang-bang” target maneuvers

This figure represents the average miss distance of 100 Monte Carlo simulation runs as a function of the timing of the reversal (switch)

in the target maneuver direction. The data used for these simulations are given in Table 1.

In the simulations DGL/1 with a typical Kalman filter augmented with a shaping filter was used. Such a shaping filter, driven by a zero mean white noise represents random target maneuvers [10]. The shaping filter selected for this case was based on an exponentially correlated acceleration (ECA) model, suggested by Singer [11]. Such a shaping filter has first order dynamics with two tuning parameters, the correlation time of the maneuver τ_s and the level of the assumed process noise, expressed by its standard deviation $\sigma_s = a_E^{max}/C_s$. In this example the parameters of the shaping filter are $\tau_s = 1.5$ sec and $C_s = 2$.

Table 1. Horizontal endgame parameters

| Parameter | Value |
|-----------------------------|---------------------------|
| Interceptor velocity | $V_P = 2300$ m/sec |
| Target velocity | $V_E = 2700$ m/sec |
| Interceptor maneuverability | $a_P^{max} = 20$ g |
| Target maneuverability | $a_E^{max} = 10$ g |
| Interceptor time constant | $\tau_P = 0.2$ sec |
| Target time constant | $\tau_E = 0.2$ sec |
| Initial endgame range | $R_0 = 20$ km |
| Endgame duration | $t_f = 4$ sec |
| Measurement noise | $\sigma_{ang} = 0.1$ mrad |
| Sampling rate | $f = 100$ Hz |

The main reason for the degraded homing performance is the inherent delay introduced by the convergence time of the estimation process. DGL/1 can correct the error created by the delay only if the change of the acceleration command occurs in the early part of the endgame. In this case sufficient time remains until intercept, the estimated acceleration converges and the guidance law receives reasonably accurate values of the zero-

effort miss distance early enough to achieve good precision.

The value of the estimation delay can be reduced by increasing the bandwidth of the estimator, which can be done by selecting other tuning parameters of the shaping filter. In this case the large miss distances associated with acceleration command changes occurring in the last phase of the endgame, at the expense of less efficient filtering that will lead to increased residual estimation errors and larger miss distances for acceleration command changes occurring in the early part of the engagement. For an improved homing performance both the estimation delay and the variance have to be reduced. A single estimator cannot satisfy both requirements.

4. Integrated Design Approach

4.1 Task separation

Since no single estimator can satisfy the requirements of homing accuracy, the different tasks performed by a classical estimator, have to be separated and assigned to different elements. The main task is the estimation of the state variables (including the target acceleration) involved in the guidance law. This task can be performed by a narrow bandwidth filter, if the correct model of the target maneuver is available. Thus, the first task to be carried out is model identification, using a multiple model structure [12]. The filters for this task should be of large bandwidth, in order to complete the model identification as fast as possible. Two basic types of target maneuver models are considered, a piecewise constant one (including the most effective “bang-bang” type evasion) and a time varying periodical maneuver.

4.2 Tuned estimators

In an earlier paper [13] a multiple model estimator, where each model assumed a different timing of the direction reversal (switch) a “bang-bang” type maneuver, is described. Using such an estimator “tuned” to the correct switch eliminates the delay and

yields excellent homing performance as it can be seen in Fig. 4 for the case of $(t_{go})_{sw} = 1.0$ sec.

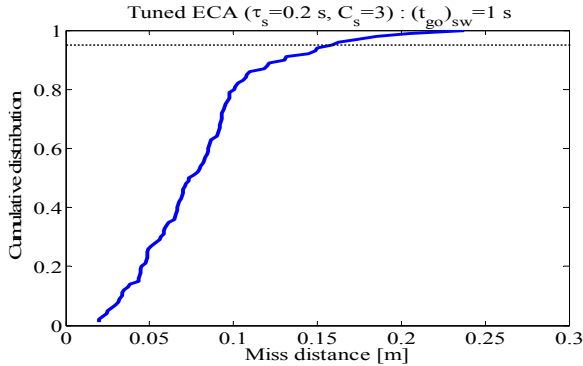


Fig. 4. Cumulative miss distance distribution with a perfectly “tuned” estimator

Even if the switch occurs shortly after the time anticipated by the estimator, good performance is obtained, as illustrated in Fig. 5 as a function of $\Delta(t_{go})_{sw}$, the difference between the “tuning time” of the estimator and the true value of $(t_{go})_{sw}$.

$$\Delta(t_{go})_{sw} = (t_{go})_{tune} - (t_{go})_{sw} \quad (23)$$

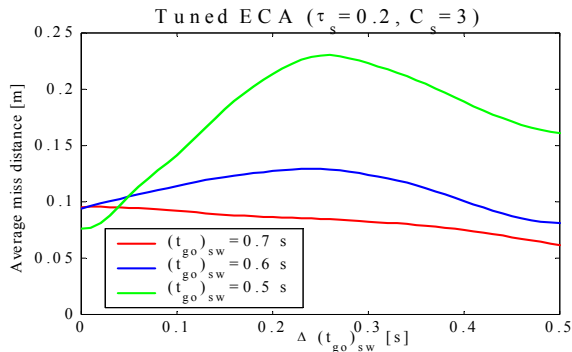


Fig 5. Average miss distances with “tuned” estimators for “bang-bang” target maneuvers

This figure shows small miss distances and a surprising robustness, allowing to use only very few “tuned” estimators for covering the range of interest. The estimators for this evaluation employ ECA shaping filters with a relatively large bandwidth ($\tau_s = 0.2$ sec, $C_s = 3.0$). Assuming that the switch in the target acceleration command can be detected sufficiently fast, this robustness property and the

results of Figs. 3 suggests to use against “bang-bang” type maneuvers the an integrated logic based estimation/guidance strategy as a function of time-to-go. Until the identification of the target maneuver type, a narrow bandwidth estimator and a guidance law (DGL/0) not using target acceleration (without the term ΔZ_E (21) in the expression (19) of the *zero effort miss distance*) are used. Once the direction of a constant maneuver has been identified, the guidance law is changed to DGL/1, preserving the same estimator. This estimator is kept until “critical” time-to-go ($t_{go} = 1.6$ sec in the present example) is reached, even if a jump in the direction of the target maneuver command is detected. For $t_{go} \leq 1.6$ sec, as a jump has been detected the narrow bandwidth estimator is replaced by the nearest (earlier) “tuned” wide bandwidth version. Three estimators “tuned” for $(t_{go})_{sw} = 1.6, 1.0, 0.5$ sec, cover the range of interest in the present example. After “jump” detection, the active estimator remains unchanged. Since the estimation delay with a “tuned” estimator is negligible, the guidance law used with these estimators is DGL/1.

This new estimation/guidance concept was tested by extensive Monte Carlo simulations for every 0.1 sec of $(t_{go})_{sw}$ within the 4 sec duration of the benchmark endgame, using 100 noise samples for each. The results, assuming *ideal* detection, are indeed excellent as shown in Fig. 6. Since an *ideal* detection of the jump in the direction of the target maneuver command is not feasible, the Monte Carlo simulations were repeated assuming small detection delays of 0.05 and 0.1 sec. The cumulative probability distributions of the miss distance for these two cases are also shown in Fig.6. A detection delay of 0.05 sec has only a minor effect, while a delay of 0.1 sec causes more important performance degradation, mainly for maneuver switches near to the end of the interception. These results strongly emphasize the need for a fast “jump detector”, which has to be developed, as an additional element of the corporate estimation system. Fig. 6 also includes the results obtained in a recent conference paper [14], already using the ideas of

task separation and the explicit application of the time-to-go in the estimation process, but employing a delay compensating guidance law denoted as DGL/C [] with "tuned" estimators and assuming an ideal "jump" detection.

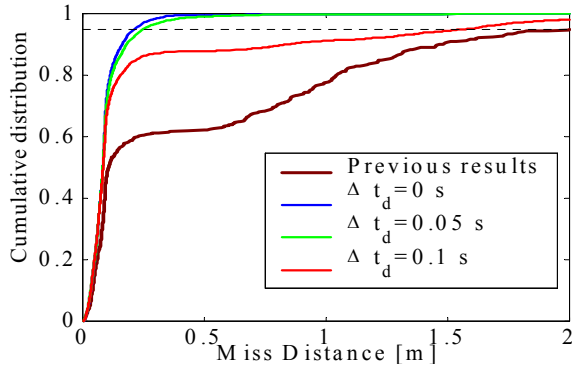


Fig. 6 Cumulative miss distance distributions with logic based "tuned" estimators

4.3 Guidance law modifications

It was observed that due to the detection delay and the remaining short time the interceptor is unable to reach its maximum lateral acceleration and correct the guidance error generated during the delay. This deficiency was corrected by increasing the lateral acceleration command for small values of time-to-go, when a maximum maneuver is needed due to the detected change of the target maneuver direction. The increase in the commanded acceleration gain is expressed for $t_{go} \leq (t_{go})_{sw}$ by

$$a_p^c = a_p^c(t_{go}, k) = \frac{a_p^{\max} \text{sign } Z}{1 - k \exp\left(-\frac{t_{go}}{\tau_p}\right)} \quad (24)$$

The parameter k is selected to satisfy

$$|a_p(t_f, k)| = a_p^{\max} \quad (25)$$

Its value depends on $(t_{go})_{sw}$ and the value of a_p at that current time-to-go. The effect of this gain enhancement is shown in Fig. 7.

Further improvement can be achieved by introducing a time varying dead in the DGL/1 guidance law for the period when the "tuned" estimators are used.

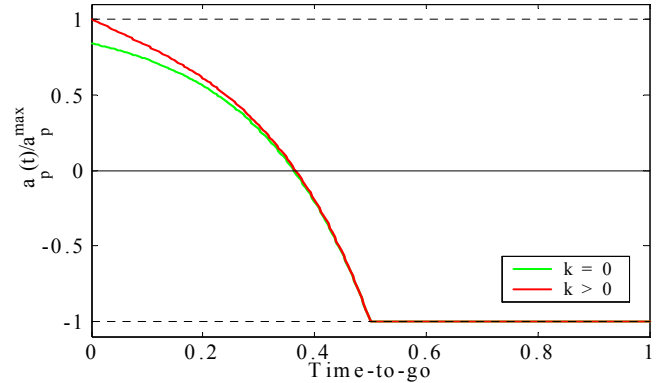


Fig. 7 The effect of gain enhancement

$$\text{sign}_{dz}(Z) = \begin{cases} 1.0, & Z > A_{dz} \exp(-b_{dz}t) \\ 0.0, & |Z| \leq A_{dz} \exp(-b_{dz}t) \\ -1.0, & Z < -A_{dz} \exp(-b_{dz}t) \end{cases} \quad (27)$$

where A_{dz} is the initial amplitude and b_{dz} is exponential decay rate of the dead zone. This modification reduces the error that occurs during the detection delay as seen in Fig. 8.

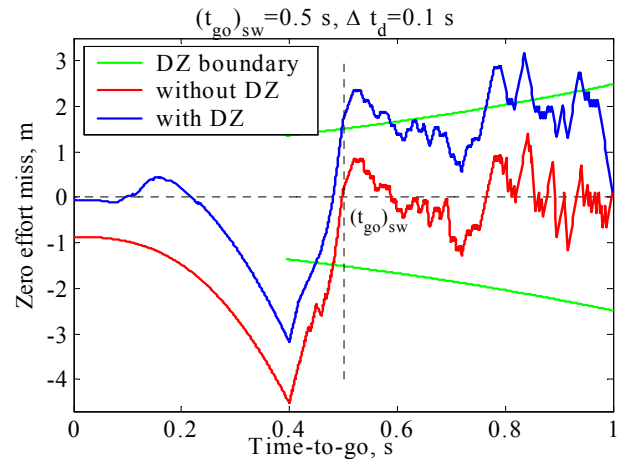


Fig. 8 The effect of the dead zone.

The dead zone is used only until the switch is detected. In the simulations the values of $A_{dz} = 50$ m and $b_{dz} = 1/\text{sec}$ were selected. The effect of the two improvements is clearly seen in Fig. 9, summarizing different figures of merit for the homing performance in the interception endgame.

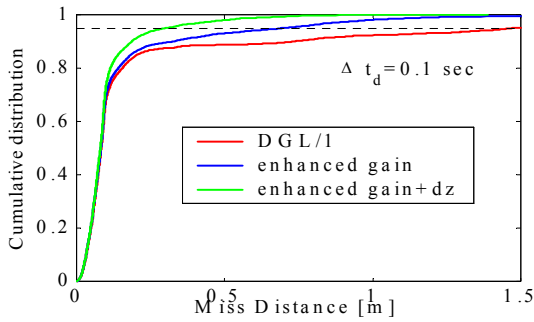


Fig. 9 Cumulative miss distance distributions with guidance law modifications

4 Validation in 3-D

4.1 Scenario Data

The new logic based estimation/guidance strategy outlined above (with enhanced terminal gain and dead-zone) was validated in a generic three-dimensional endo-atmospheric BMD scenario, described in the sequel. It is an endo-atmospheric interception scenario between altitudes of 20-30 km with an initial "lock-on" range of 20 km.

The target is a generic tactical ballistic missile with aerodynamic control, performing either spiral or horizontal bang-bang evasive maneuvers. It is assumed to be launched from the distance of 600 km on a minimum energy trajectory. It is characterized by a ballistic coefficient $\beta=5000 \text{ kg/m}^2$ and a trimmed lift-to-drag ratio $\Lambda = 2.6$. Its velocity at reentry of an altitude of 150 km is $V_{e0}=1720 \text{ m/s}$ with a flight path angle of $\gamma_{e0} = -18^\circ$ and a horizontal distance from target of 210 km.

The interceptor is generic two-stage solid rocket missile with a specific impulse of $I_{sp} = 250 \text{ sec}$ and has two identical guidance channels for aerodynamic control (skid to turn). The propulsion, mass and aerodynamic data of the two stages are summarized in Table 2.

Table 2. Interceptor data

| | t_b [sec] | T [kN] | m_0 [kg] | SC_D [m^2] | $SC_{L,ma}$ x [m^2] |
|-----------------------|----------------|-----------|---------------|----------------------------|-----------------------------------|
| 1 st stage | 6.5 | 229 | 1540 | 0.10 | 0.24 |
| 2 nd stage | 13 | 103 | 781 | 0.05 | 0.20 |

It is assumed that the interceptor is launched in a point defense task precalculating the firing solutions for different interception altitudes. The ignition delay of the second stage is timed to guarantee interception with longitudinal acceleration and not decreasing maneuverability. The speed profiles for the interception altitudes are shown in Fig. 10.

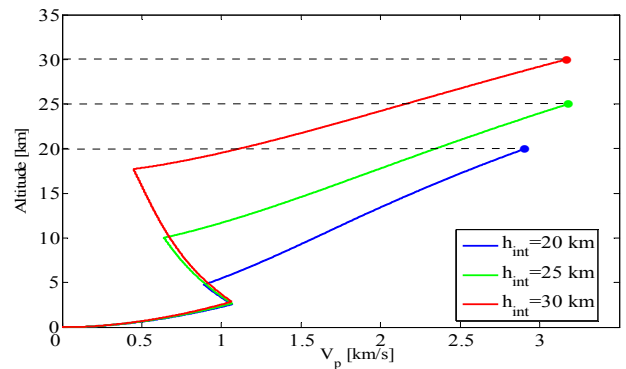


Fig. 10 Interceptor velocity profiles

During the endgame the maneuverability of the target is monotonically increasing leading to a monotonically decreasing value of μ seen in Fig. 11. The time constants of the interceptor and the target, as well as the measurement noise and the sampling rate, are the same as in planar case summarized in Table 1.

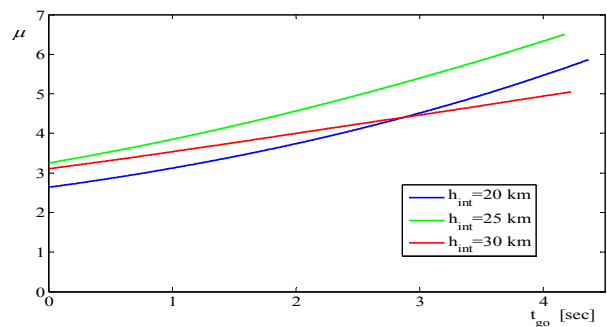


Fig. 11 Endgame maneuverability ratio

4.2 Simulation philosophy

All the simulated endgame engagements had a slightly longer duration than 4 sec. The estimation and guidance strategy in these scenarios was based on the assumption that the reentering TBM can execute one of the following types of maneuvers:

- (1) Spiral (random phase) evasive maneuvers with unknown roll rate.
- (2) Horizontal bang-bang evasive maneuvers with randomly timed reversal.

Accordingly, the first second of the endgame is devoted to discriminate between the two maneuver types. During an additional second the roll rate range (for 1) or maneuver direction (for 2), as well as the magnitude, are estimated. Until target maneuver identification a narrow band estimator and a guidance law, both assuming no target maneuver, are used. If spiral maneuver is identified the closest periodical estimator is selected. If the identified maneuver is more or less constant (or varying slowly) the logic-based scheme developed for the planar case including the guidance law modifications are used. After target maneuver identification DGL/E with the output of the estimator is used.

4.3 Simulation Results

The validation effort is limited to the following cases: (i) homing accuracy against random horizontal bang-bang maneuvers (using the logic based scheme) at different interception altitudes; (ii) homing accuracy against spiral target maneuvers of different frequencies (p_0), (using matched and unmatched periodical estimators) at the interception altitude of 25 km. Homing accuracy statistics, presented in the following figures, are expressed by the cumulative miss distance distributions based on 1000 Monte Carlo simulation runs for each scenario, assuming Gaussian noise and uniform phase or reversal time (switch) distributions.

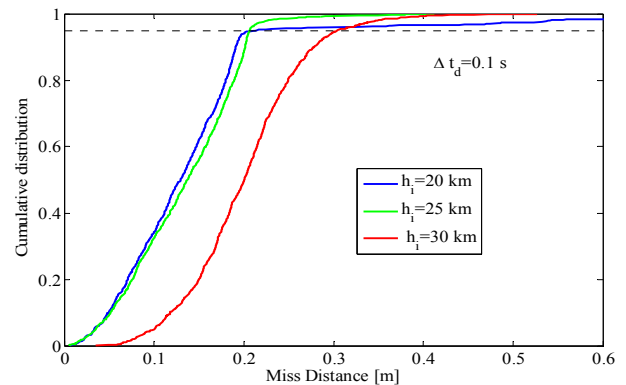


Fig. 12 Homing accuracy against random horizontal bang-bang maneuvers

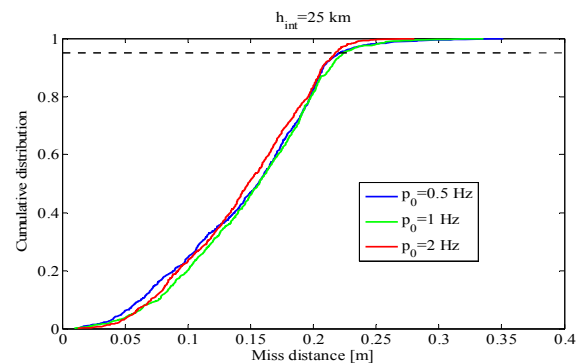


Fig. 13 Homing accuracy against random phase spiral maneuvers (matched periodical estimators)

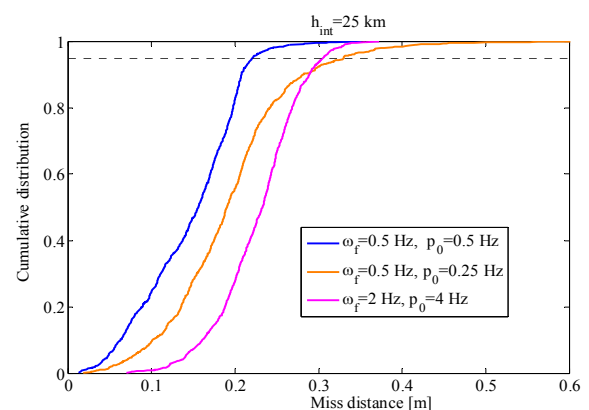


Fig. 14 Homing accuracy against random phase spiral maneuvers (unmatched periodical estimators)

5 Conclusions

The simulation results presented in the figures clearly confirm the validity of the integrated estimation/guidance approach, which was developed using a simplified planar constant speed model, in a generic, but realistic theatre ballistic missile defense scenario. The homing accuracy, using generic target and interceptor models, in a realistic three-dimensional interception scenario is similar to the accuracy found in the simplified planar model.

The simulations clearly demonstrated that the integrated estimation/guidance approach not only leads to a substantial homing accuracy improvement compared to earlier results but has also the potential to satisfy the "hit-to-kill" requirement against two types of stressing evasive target maneuvers.

The applicability of the new design approach is twofold: (i) upgrading the homing performance of existing interceptors without requiring hardware modifications; (ii) designing new cost effective interceptors with reduced hardware requirements.

6 References

- [1] Hughes, D., "Next Arrow test this summer after scoring direct hit", *Aviation Week & Space Technology*, March 24, 1997.
- [2] Philips, H. E., "PAC-3 missile seeker succeeds" *Aviation Week & Space Technology*, March 22, 1999.
- [3] Shinar, J. and Zarkh, M. "Interception of maneuvering tactical ballistic missiles in the atmosphere", *Proceedings of the 19th ICAS Congress*, Anaheim, CA, 1994, pp.1354-1363.
- [4] Shinar, J. and Shima, T., "Kill probability assessment against maneuvering tactical ballistic missiles", AIAA 10th Multinational Conference on Theater Missile Defense, Eilat, Israel, June 1997.
- [5] Zarchan, P. *Tactical and strategic missile guidance*, Vol. 124 in Progress in Astronautics and Aeronautics Series, 1990, AIAA, Inc. Washington D.C.
- [6] Shinar, J. Turetsky, V. and Oshman, Y. "New logic-based estimation/guidance algorithm for improved homing against randomly maneuvering targets", *Proceedings of AIAA Guidance, Navigation and Control Conference*, Providence, RI, August 2004.
- [7] Shinar, J. "Solution techniques for realistic pursuit-evasion games", in *Advances in Control and Dynamic Systems*, (C.T. Leondes, Ed.), Vol. 17, pp. 63-124, Academic Press, N.Y., 1981.
- [8] Shima, T. and Shinar, J. (2002) "Time varying linear pursuit-evasion game models with bounded controls", *Journal of Guidance, Control and Dynamics*, Vol. 25, No.3, pp. 425-432.
- [9] Glizer, V. Y. and Shinar, J. "Optimal evasion from a pursuer with delayed information", *Journal of Optimization Theory and Applications*, Vol.111, No. 1, 2001, pp. 7-38.
- [10] Zarchan, P. Representation of realistic evasive maneuvers by the use of shaping filters, *Journal of Guidance and Control*, Vol. 2, No.1, 1979, pp. 290-295.
- [11] Singer, R. A., "Estimating optimal filter tracking performance for manned maneuvering targets", *IEEE Trans. on Aerospace and Electronic Systems*, Vol. ES-6, No. 4, 1970, pp. 473-483.
- [12] Bar-Shalom, Y. and Xio-Rong, L., "*Estimation and tracking: principles, techniques, and software*", Artech House, 1993.
- [13] Shima, T., Oshman, Y. and Shinar, J. "An efficient application of multiple model adaptive estimation in ballistic missile interception scenarios", *Journal of Guidance, Control and Dynamics*, Vol.25, No. 4, 2002, pp. 667-675.
- [14] Shinar, J., Oshman, Y., Turetsky, V., and Evers, J. "On the need for integrated estimation/guidance design for hit-to-kill accuracy", *Proceedings of the 2003 American Control Conference*, Denver, CO, June 2003.
- [15] Shinar, J. and Shima, T. "Non-orthodox guidance law development approach for the interception of maneuvering anti-surface missiles", *Journal of Guidance, Control and Dynamics*, Vol.25, No. 4, 2002, pp. 658-666.